# Stochastic Power System Dynamic Simulation and Stability Assessment Considering Dynamics From Correlated Loads and PVs

Ketian Ye<sup>®</sup>, Student Member, IEEE, Junbo Zhao<sup>®</sup>, Senior Member, IEEE, Nan Duan<sup>®</sup>, Senior Member, IEEE, and Daniel Adrian Maldonado<sup>®</sup>, Member, IEEE

Abstract—The integration of uncertain photovoltaics (PVs) and flexible loads leads to uncertainties in the power system dynamic simulation results. Furthermore, geographically close PV farms are correlated and may exhibit nonlinear correlations. This article proposes a copula-based sparse polynomial chaos expansion (PCE) framework for quantifying the impacts of uncertain dynamic PVs and loads on power system dynamic simulations and stability. The dynamics include both PV and load stochasticity and those governed by differential and algebraic equations. The copula statistics are utilized to accurately characterize the dependence structure of PVs and further used to develop the copula-PCE for quantifying the impacts of uncertain PVs and loads. A probabilistic TSI is also developed to assess the uncertainties from PVs and loads on the system stability. To address the cases, where both stable and unstable conditions coexist, a preprocessing step via sample classification is proposed. The effects of different dependence structures of PVs and different numbers of uncertain sources are investigated. Comparison results with other methods on the modified IEEE 39and 118-bus systems, including the Monte Carlo method, Latin hypercube sampling, and traditional PCE without consideration of uncertain input correlations show that the proposed method is able to accurately quantify the uncertain dynamic simulations and transient system stability while being computationally efficient.

*Index Terms*—Copula statistics, dynamic photovoltaics (PVs), nonlinear correlations, polynomial chaos expansion, power system dynamics, uncertainty quantification.

#### NOMENCLATURE

#### Abbreviations

DERs Distributed energy resources. LHS Latin hypercube sampling.

Manuscript received 17 April 2022; revised 9 June 2022; accepted 27 July 2022. Date of publication 1 August 2022; date of current version 21 November 2022. Paper 2022-IACC-0503.R1, presented at the 2021 IEEE/IAS Industrial and Commercial Power System Asia (I&CPS Asia), Chengdu, China, Jul. 18–21, and approved for publication in the IEEE TRANSACTIONS ON INDUSTRY APPLICATIONS by the Industrial Automation and Control Committee of the IEEE Industry Applications Society. This work was supported in part by National Science Foundation under Grant ECCS 1917308 and in part by the Department of Energy Advanced Grid Modernization program. (Corresponding author: Junbo Zhao.)

Ketian Ye and Junbo Zhao are with the Department of Electrical and Computer Engineering, University of Connecticut, Storrs, CT 06269 USA (e-mail: ketian.ye@uconn.edu; junbo@uconn.edu).

Nan Duan is with the Lawrence Livermore National Laboratory, Livermore, CA 94550 USA (e-mail: duan4@llnl.gov).

Daniel Adrian Maldonado is with the Argonne National Laboratory, Lemont, IL 60439 USA (e-mail: maldonadod@anl.gov).

Color versions of one or more figures in this article are available at https://doi.org/10.1109/TIA.2022.3195475.

Digital Object Identifier 10.1109/TIA.2022.3195475

MAPE Mean absolute percentage error.

MC Monte Carlo.

MCS Monte Carlo simulation.
PCE Polynomial chaos expansion.
PDF Probability density function.

PV Photovoltaic.

RT Rosenblatt transformation.
TSI Transient stability index.

#### Power System Dynamics

ξ Uncertain resources.

u System input.x Dynamic state variables.

y Algebraic state variables.

 $\delta_{max}$  Maximum rotor angle difference between genera-

tors.

 $\mathcal{M}$  Dynamic model. t Simulation time.

#### PCE and Copula

Regularization parameter.

 $\mu_s$  Mean value of model response in stable case.  $\mu_{us}$  Mean value of model response in unstable case.

 $\omega$  Quadrature weights.

 $\Psi$  PCE basis.

 $\sigma_s^2$  Variance of model response in stable case. Variance of model response in stable case.

a PCE coefficient.d Input dimension.

 $F_k$  Joint cumulative distribution function of k.

 $F_{k|1,\ldots,k-1}$  this.

n PCE degree.X Model output.

Z Model input, decoupled uncertain resources.

#### I. INTRODUCTION

HE uncertainties from dynamic loads and distributed energy resources (DERs), such as photovoltaics (PVs) can be propagated through dynamic models, leading to uncertainties in power system dynamic responses. These uncertainties, if not properly quantified, would result in a wrong judgment on power system stability, and consequently, improper preventive controls. The PV and load dynamics mean that they are governed by differential and algebraic equations. This is different from the

0093-9994 © 2022 IEEE. Personal use is permitted, but republication/redistribution requires IEEE permission. See https://www.ieee.org/publications/rights/index.html for more information.

stochasticity from PVs and loads that are affected by changing weather conditions or load variations. The necessity of quantifying and monitoring such uncertainty motivates the investigation for appropriate quantitative measures that can provide statistics information of model responses.

To quantify the uncertainties from dynamic PVs and loads on the power system dynamic simulations, analytical methods have been proposed [1]–[3]. They are based on model linearization, simplification, and abstraction. These approximations may lead to unexpected errors. A more traditional way of quantifying the impacts of uncertain sources on power system dynamic responses is to use the Monte Carlo simulations (MCS) and its enhanced variants [4]–[7]. However, the high computational cost of MCS hinders its application on practical large-scale systems with a large number of uncertain loads and DERs. It is, therefore, important to develop computationally efficient alternatives. Taking the Latin hypercube sampling (LHS), for example, it needs a smaller dataset to obtain a reasonable accuracy as compared to the MCS but has computational difficulties for larger-scale systems. Indeed, the consideration of dynamic PVs and loads significantly increases the complexity of the model, and thus, LHS is subject to heavy computational burden. Another way is to perform analysis on the response of interest [8]–[10]. In [8], the method of moments (MoM) and automatic differentiation are leveraged to quantify the uncertainty propagation of states and parameters in dynamic simulations by propagating the first few moments. But the estimates of MoM may be insufficient due to moment closure problem and the computational efficiency is limited. As a widely used tool for dynamic system analysis, the trajectory sensitivity analysis has been applied to power system dynamic simulation [9] and dynamic security assessment [10]. Yet, the trajectory sensitivities are calculated based on partial derivatives, and therefore, it is insufficient when severe nonlinearity of the system exists. The surrogate modeling method is also an option as the statistics of the output of interest can be estimated; for example, the stochastic averaging [11]. Second-order Taylor series and third-order normal form approximations are developed in [9] and [12]. In [13], Kalman filter and unscented transformation are employed to provide an estimation of the distribution of the transient stability margin. The shortages of unscented transformation include high computational burden due to Cholesky factorization at every step and Gaussian noise assumption. Polynomial chaos expansion (PCE) and the related stochastic collocation methods can yield the corresponding statistical information from their coefficients for uncertainty quantification. The existing PCE-based methods applied in power system dynamics [14], [15] consider only independent input variables but the power injections from PVs at geographically close locations are usually correlated [16]. The correlations between uncertain inputs can significantly affect the power system dynamic process and have not been considered in the literature. Furthermore, they are unable to deal with the cases, where the uncertainties may lead to simultaneous stable and unstable system responses with different probabilities.

This article extends our previous work on using PCE for probabilistic analysis [17], [18] to power system dynamic simulations and develops the probabilistic transient stability index (TSI) to assess the uncertainties from dynamic PVs and

loads on the system stability. The key idea is to leverage the copula statistics to capture the nonlinear correlations among uncertain dynamic PVs and loads so that the sparse PCE can be extended for uncertainty quantification of dynamic simulations. A preprocessing strategy is also developed for handling the coexistence of stable and unstable cases in the probabilistic transient stability assessment. It has the following contributions.

- It can quantify the uncertainty propagation during power system dynamic simulations considering different uncertain input distributions and correlations, including both linear and nonlinear correlations. The copula-PCE for probabilistic power flow [17] has been extended to deal with dynamic equations. We transform the dynamic process into uncertainty quantification for each time step. This allows us to take advantage of the static copula-PCE formula and to calculate the confidence intervals of power system dynamic responses at each time instant. A sparse version of copula-PCE is also developed to further increase computational efficiency.
- 2) As compared to [18], this work can handle stable and unstable conditions as well as the coexist of stable and unstable scenarios caused by uncertain inputs. This is achieved via a preprocessing strategy, where the dynamic responses are categorized into stable and unstable conditions based on the TSI. Then, PCE models are constructed for them, respectively, to calculate the statistics of dynamic model responses. This is very important to accurately calculate the probabilistic TSI and quantify the probabilities of being stable and unstable, respectively.
- Existing PCE approaches for power system dynamic simulations have neglected the dynamics from dynamic loads and PVs [18]. Our proposed approach is general to deal with them efficiently.
- 4) Comparison results with MCS, LHS, and traditional PCE without consideration of uncertain input correlations show that the proposed method is able to accurately quantify the uncertain dynamic simulations and transient system stability while being much more computationally efficient. It is also shown that when the dynamics of PVs and loads are considered, LHS and MCS have significantly increased computational burden, which is not the case for our proposed method.

The rest of this article is organized as follows. Section II shows the problem statement. Section III presents the proposed framework and its implementation. Section IV shows the simulation results, and finally, Section V concludes this article.

#### II. PROBLEM STATEMENT

The power system dynamic model with uncertain loads and PVs can be expressed by the following stochastic differential and algebraic equations (DAEs) [15]:

$$\begin{cases} \dot{x} = f(x, y, u, \xi) \\ \mathbf{0} = g(x, y, \xi) \end{cases}$$
 (1)

where  $f(\cdot)$  and  $g(\cdot)$  are vector-valued functions; x and y, respectively, denote the dynamic state vector and the algebraic state vector containing algebraic variables, such as bus voltage

magnitudes and angles; u is the system input; and  $\xi$  is a random vector that represents all uncertain resources. In this article, the uncertainties come from power injections of flexible loads and uncertain PVs, resulting in uncertain power system dynamic simulations.

This article aims to investigate the impacts of uncertain dynamic loads and PVs on power system dynamic simulations and transient stability. Let the relationship between random vector  $\boldsymbol{\xi}$  and model response

$$x(t) = \mathcal{M}(\xi, t) \tag{2}$$

where  $\xi$  represents uncertainties from loads and PVs; x includes generator dynamic variables, such as rotor speeds and angles that are used for transient stability assessment. The target is to quantify the uncertainty propagation from  $\xi$  to x through the nonlinear model  $\mathcal{M}$  derived from DAEs. By quantifying the uncertainty propagation through the power system dynamic model, the statistics of model responses can indicate how the variability of uncertain resources affects the system dynamics. The detailed information, such as upper and lower bounds of dynamic responses can be used for stability analysis and control.

The most widely used method is the MCS, where a large number of samples are drawn from probability distribution of  $\xi$ . For each sample, the power system dynamic simulation is performed to obtain the path of the desired model response. Based on all sample responses, the statistics, such as mean and variance are computed. However, MCS is computationally inefficient for a large-scale system with a large number of uncertain inputs. Furthermore, geographically close uncertain PVs are correlated, exhibiting even nonlinear correlations [16]. The existing works do not consider the impacts of nonlinear correlations on stochastic dynamic simulations. Furthermore, there is a lack of research in quantifying the probabilities of losing stability when uncertain sources may lead to both stable and unstable scenarios. This article proposes a copula-based sparse PCE framework to deal with these challenges with a high computational efficiency.

### III. PROPOSED DYNAMIC SIMULATION UNCERTAINTY QUANTIFICATION FRAMEWORK

The proposed framework contains uncertain source distribution and dependence structure inference, PCE model construction, dynamic simulation uncertainty quantification, and probabilistic stability index calculation. They are shown as follows.

#### A. PCE for Dynamic Simulation Uncertainty Quantification

PCE is a widely used approach for uncertainty quantification in different domains [19]. By representing random variables or processes in terms of orthogonal polynomials, PCE is able to provide analytical calculations of model response statistics. It should be noted that, unlike the static problem, the model responses for dynamic systems are time-dependent, and as a

result, the statistics of model responses evolve as a function of time

To this end, a set of orthogonal polynomials are adapted with respect to the changing statistics. The aforementioned desired model response shown in (2) can be represented by a polynomial function of  $\mathcal{E}$  by the following expansion [20]:

$$x(t) = \sum_{i=1}^{\infty} a_i(t) \Psi_i(\boldsymbol{\xi})$$
 (3)

where  $\boldsymbol{\xi} \in \mathcal{R}^d$  is uncertain input vector,  $\boldsymbol{\Psi}_i$  and  $a_i(t)$  denote the orthogonal basis and its corresponding coefficient with respect to  $\boldsymbol{\xi}$ . The orthogonal basis  $\boldsymbol{\Psi}_i$  is constructed based on the distributions of uncertain inputs. In practice, a truncation is often performed on (3), yielding [20]

$$x \approx \sum_{i=1}^{N_p} a_i(t) \Psi_i(\boldsymbol{\xi}) \tag{4}$$

where  $N_p = (d+n)!/(d!n!) - 1$ ; d is the number of random variables; and n is the degree of the truncated polynomial function. Classical univariate orthonormal polynomials for commonlybused distributions include Legendre polynomials for Uniform distribution, Hermite for Gaussian, Jacobi for Beta, etc. [19]. For arbitrary distributions, the orthogonal polynomials are obtained using the Stieltjes procedure [19], which computes the basis numerically through the recurrence relation between bases. Based on that, the multivariate polynomials are then constructed as the tensor product of these univariate components. Basis truncation can be further applied to reduce the computational burden by excluding basis terms that are less important [21]. Subsequently, the PCE coefficient calculation can be achieved via the projection method or regression method [21]. The Gaussian quadrature-based projection method computes the polynomial coefficients following the definition of PCE and the orthogonality property of polynomial basis [21], i.e.,

$$a_{i}(t) = \int_{\Omega_{\xi}} \mathcal{M}(\boldsymbol{\xi}, t) \boldsymbol{\Psi}(\boldsymbol{\xi}) f(\boldsymbol{\xi}) d\boldsymbol{\xi}$$

$$\approx \sum_{n=1}^{N} \omega^{(n)} \mathcal{M}(\boldsymbol{\xi}^{(n)}, t) \boldsymbol{\Psi}_{i}(\boldsymbol{\xi}^{(n)})$$
(5)

where a set of weights  $\omega^{(n)}$  and quadrature points  $\boldsymbol{\xi}^{(n)}$  are derived from Lagrange polynomial interpolation;  $f(\cdot)$  is the probability distribution of uncertain input;  $\mathcal{M}(\boldsymbol{\xi}^{(n)},t)$  represents the desired realizations from the power system dynamic simulation. The numerical evaluation of integrals requires a set of N collocation points and the corresponding model responses. Regression method, on the other hand, computes the coefficients by minimizing the following objective function:

$$\widehat{\boldsymbol{a}}(t) = \arg\min E[(\boldsymbol{x}^T \boldsymbol{\Psi}(\boldsymbol{\xi}) - \mathcal{M}(\boldsymbol{\xi}, t))^2]. \tag{6}$$

To deal with high-dimensional input, the sparse techniques can be used [21]. This article adopts the least angle regression algorithm by introducing a regularization term

$$\widehat{\boldsymbol{a}}(t) = \arg\min E[(\boldsymbol{x}^T \boldsymbol{\Psi}(\boldsymbol{\xi}) - \mathcal{M}(\boldsymbol{\xi}, t))^2] + \lambda \|\boldsymbol{x}\|.$$
 (7)

As one of the advantages, the statistics of the PCE model outputs are embedded in its coefficients. In particular, the mean and the variance of PCE for each timestep can be estimated as

$$E[\boldsymbol{x}(t)] = \boldsymbol{a}_0 \quad \text{var}[\boldsymbol{x}(t)] = \sum_{i=1}^{N_p} a_i^2(t) E[\boldsymbol{\Psi}_i^2]. \quad (8)$$

Note that  $E[\Psi_i^2] = I$  for the orthonormal basis. Such estimation is much more efficient than calculating them from sampling-based approaches, such as MCS. Once the PCE model is constructed, the statistical information estimates (mean and variance) can be analytically calculated from PCE coefficients. This analytical calculation is based on the orthogonality of the PCE basis, and thus, is very fast.

#### B. PCE Considering Correlated Uncertain Inputs

The conventional way of constructing PCE basis requires that the random vector  $\boldsymbol{\xi}$  is independent and its distribution is known. However, the distributions of uncertain inputs are generally unknown and it is found that the geographically close PVs have correlations, even exhibiting nonlinear correlations [16]. Specific modifications are required to maintain the orthogonality property when constructing the PCE model. To deal with unknown distributions as well as nonlinear correlations among uncertain inputs, copula statistics and Rosenblatt transformation (RT) are integrated. Specifically, copula is employed to infer the distribution of uncertain inputs and their dependence structure, while RT is utilized to establish the transformation of dependent input to independent one. This allows the PCE to preserve orthogonality condition for analytical estimate calculation.

Copula statistics have the ability to capture the complex dependence structures among random variables [22]. The representation for multivariate distribution is general and flexible by defining the marginals and the copula types that describe how the marginals are coupled. According to Sklar's theorem, for a d-dimensional continuous random variable  $\boldsymbol{\xi} = [\xi_1, ..., \xi_d]$  with marginals  $F_1, ..., F_d$  and joint cumulative distribution function (CDF),  $F_{\boldsymbol{\xi}}$ , there exists a copula function C satisfying

$$F_{\xi}(\xi_1, \dots, \xi_d) = C(F_1(\xi_1), \dots, F_d(\xi_d)).$$
 (9)

The conditional distribution function is calculated by [23]

$$F_{j|\mathcal{A}}(\xi_j|\boldsymbol{\xi}_{\mathcal{A}}) = \frac{\partial C_{j,i|\mathcal{A}\setminus\{i\}}(F(\xi_j|\boldsymbol{\xi}_{\mathcal{A}\setminus\{i\}}), F(\xi_i|\boldsymbol{\xi}_{\mathcal{A}\setminus\{i\}}))}{\partial F(\xi_i|\boldsymbol{\xi}_{\mathcal{A}\setminus\{i\}})}$$
(10)

where  $j \in \mathcal{A}, i \in D \setminus \mathcal{A}$ ;  $\mathcal{A}$  denotes a subset of indices  $D = \{1, \ldots, d\}$  and  $\mathcal{A} \setminus \{i\}$  denotes excluding ith component;  $F_{j|\mathcal{A}}$  is the CDF of the random variable  $\xi_j$  conditioned on  $\xi_{\mathcal{A}}$ ; and  $C_{j,i|\mathcal{A}}$  represents the copula function of the jth component given  $\mathcal{A}$ . Canonical vine (C-vine) copula is utilized to tackle input vector with high dimensions [22].

Upon the construction of copula structure, RT is established, where the dependent random vector  $\boldsymbol{\xi}$  is first transformed into

independent ones z via

$$RT: \boldsymbol{\xi} \to \boldsymbol{z} = \begin{cases} F_1(\xi_1) \\ \dots \\ F_{k|1,\dots,k-1}(\xi_k|\xi_1,\dots,\xi_{k-1}) \\ \dots \\ F_{d|1,\dots,d-1}(\xi_d|\xi_1,\dots,\xi_{d-1}) \end{cases}$$
(11)

where  $F_{d|1,...,d-1}$  is the CDF of the conditioned random variable  $\xi_d|\xi_1,\ldots,\xi_{d-1}$ .

In this way, PCE constructs the model of the relationship between z and model response X that captures the nonlinear dependence while maintaining the orthogonality of basis. Similarly, new inputs  $\hat{\xi}$  should be first transformed into  $\hat{z}$  and further leveraged by PCE for model response prediction and uncertainty quantification.

#### C. Handling Coexistence of Stable and Unstable Scenarios

When the system is operated under stressed conditions or subject to large disturbances, the perturbations on DAE state initialization caused by uncertainties from dynamic loads and PVs can lead to stable, unstable, and coexistence of stable and unstable scenarios with different probabilities. Since the patterns for absolute stable and unstable scenarios are quite different, it is not feasible to use one PCE model to capture the coexistence of stable and unstable scenarios, which will be shown in the numerical results section.

To address that, a data processing strategy is proposed for the samples generated from inferred PDFs of uncertain inputs. In particular, a number of samples obtained by LHS are first generated. Then, these samples are propagated via the power system DAEs to get corresponding responses. If the TSI is beyond a preset value, the corresponding sample will be claimed as unstable. Detailed explanations are shown in the next subsection. This means that a simple classification of the samples with boundary via k-means algorithm or support vector machine can be used to classify the samples into stable and unstable cases. Then, two PCE models are constructed separately using stable and unstable samples for uncertainty quantification. Note that when the system is absolutely stable or unstable, only one PCE model is needed.

#### D. Probabilistic TSI

An immediate application of uncertainty quantification for power system dynamic simulations is the probabilistic assessment of transient stability. This is critical especially for the case, where both stable and unstable scenarios exist. By providing the probability for losing the system stability to the operator, an enhanced system situational awareness can be achieved. For example, if the system is found to have a low probability of losing stability due to uncertain loads and PVs, the system operator may not want to redispatch the generators with increased costs as the risk is low. By contrast, if the probability of losing instability is high (depending on the threshold set by operators), they have to make preventive control plans via generation redispatch or load shedding. The probabilistic TSI allows the operator to have

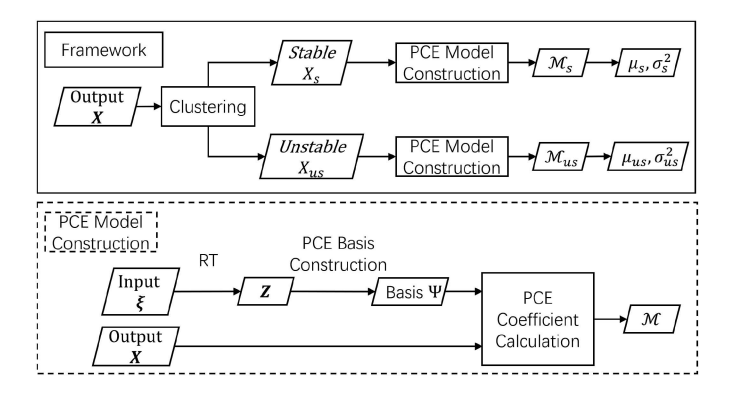


Fig. 1. Proposed copula-based PCE to quantify the uncertainties of power system dynamic simulations with correlated uncertain inputs, where  $\mu_s$  and  $\sigma_s^2$  are the mean and variance of the generator rotor angles under the stable cases. While  $\mu_{us}$  and  $\sigma_{us}^2$  denote the mean and variance of the generator rotor angles under system instability cases.

enhanced situational awareness and balance the tradeoff between system risk and costs.

A widely used TSI [25] is

$$TSI = 100 \times \frac{360 - \delta_{max}}{360 + \delta_{max}}$$
 (12)

where  $\delta_{max}$  is the maximum rotor angle difference between any two generators. When TSI>0, the system is transient stable, while TSI<0 means system unstable. The boundary is TSI=0. Note that the increase of TSI reflects transient stability enhancement and vice versa. Note that the uncertain PVs and loads are the inputs to the model, and generator rotor angles are the model output for stability assessment. The uncertainties of dynamic PVs and loads will be propagated to generator rotor angles through DAEs. The stability assessment is based on the generator rotor angles, and thus, the impacts of uncertain dynamic PVs and loads are considered.

With the constructed PCE model  $x(t) = \mathcal{M}(\xi, t)$ , we can sample  $\xi$  via Latin hypercube sampling approach to obtain a series of generator rotor angle responses, which are used to calculate the corresponding  $\delta_{\text{max}}$  and TSI. Then, a nonparametric inference method based on a kernel density estimator is used to infer the closed-form univariate PDF of TSI, i.e.,

$$\widehat{f}(TSI) = \frac{1}{mh} \sum_{i=1}^{m} K\left(\frac{TSI - TSI_i}{h}\right)$$
 (13)

where m is the number of samples; h is the bandwidth parameter that can be obtained via  $1.06\sigma m^{-0.2}$  [26] and  $\sigma$  is the estimated sample standard deviation; and K is a nonnegative kernel function, i.e., standard Gaussian kernel here.

#### E. Algorithm Implementation

The proposed method is shown in Fig. 1 and the main steps for the proposed method implementations are as follows.

1) Step 1: Inference of the uncertain input distribution and complicated correlation relationships using copula statistics.

- 2) *Step 2:* Perform dynamic simulation based on the inputs sampled from the inferred probability distribution in Step 1 and classify the response samples into two groups, i.e., stable and unstable.
- 3) *Step 3:* Construct PCE basis with RT (11), and then, calculate PCE coefficients based on samples from Step 2 using the regression method as shown in (6).
- 4) Step 4: The analytical form of statistics of model responses can be directly obtained via (8). The statistical information of both stable and unstable cases can be obtained from its coefficients thanks to the orthogonality of the polynomial basis
- 5) *Step 5:* Probabilistic TSI calculation and PDF estimation. *Remark:* The proposed method infers the probabilistic distribution of uncertain inputs considering nonlinear correlations and develops the sparse PCE to construct a reduced model of the complex physical model. This leads to the following two advantages:
  - 1) reduced number of sampling requirements;
  - speed up the simulation for each sample due to reduced model.

#### IV. NUMERICAL RESULTS

Simulations are conducted on both IEEE 39-bus and 118-bus systems with PVs. Each synchronous generator is assumed to be the two-axis model equipped with the IEEE-DC1A exciter and the TGOV1 turbine governor. The DAEs for the generator mode are shown in the Appendix. The parameters of the generator model can be found in [24]. For the 39-bus system, a three-phase fault is applied at bus 16 at 0.5 s and is cleared after ten cycles by opening line 16-24. The uncertain sources are flexible loads and PVs, and the rotor angles and speeds are selected as dynamical model responses. Three approaches are compared, i.e., LHS, PCE used in [15] without consideration of input correlations, and the proposed method, termed as CoPCE. All simulations are performed using MATLAB with 2.60-GHz Intel Core i7-6700HQ. In the simulations, loads and PVs are assumed to follow certain distributions with means being the original values and standard derivations being a certain portion (uncertainty level) of means. The performance for the uncertain information estimation is evaluated using the mean absolute percentage error (MAPE), of which the general formula is

$$MAPE = \frac{1}{T} \sum_{i=1}^{T} \left| \frac{\boldsymbol{\theta}_{i}^{*} - \hat{\boldsymbol{\theta}}_{i}}{\boldsymbol{\theta}_{i}^{*}} \right| \times 100\%$$
 (14)

where  $\theta_i^*$  and  $\theta_i$  represent the true and estimated values at time step i for all generators, respectively. More specifically, MAPEs of the mean and variance over the entire simulation time range are utilized as error indices, denoted as  $e_{\mu}$  and  $e_{\sigma^2}$ . The rotor angles have been widely used for transient stability assessment. As shown in (12), the rotor angle determines the stability condition. Due to the space limitation, we could not show all rotor trajectories for all generators and  $\delta_{2-1}$  (the rotor angle of generator 2 with respect to reference generator 1) is used as an example for illustration purposes. The benchmark is

TABLE I
DISTRIBUTIONS OF LOADS AND PVS WITH LINEAR CORRELATIONS
FOR SCENARIOS 1 AND 2

Scenarios	Scenario 1	Scenario 2
PL (MW)	$\mathcal{N}(PL, (0.1PL)^2)$	$\mathcal{N}(PL, (0.1PL)^2)$
PV (MW)	$100 \times \text{Beta } (2.06, 2.2)$	$100 \times \text{Beta } (2.06, 2.2)$
Coefficients ρ	[0.4, 0.4, 0.4]	[0.6, 0.6, 0.6]

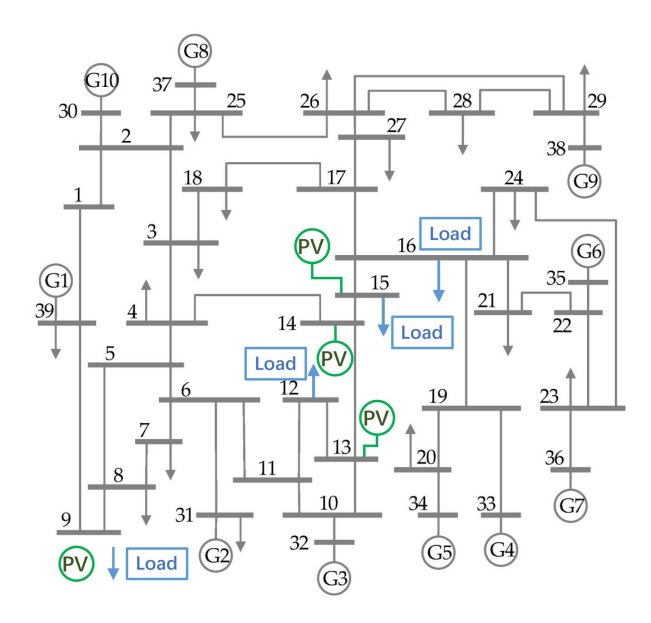


Fig. 2. Single line diagram of the IEEE 39-bus system with PVs.

obtained based on MCS with 10000 samples. The number of samples for the LHS method is 3000.

#### A. Impacts of Uncertain Inputs With Linear Correlations

This section investigates the impacts of uncertain PVs with linear correlations on rotor angle responses. Loads are assumed to be independent because they are geographically far in the transmission systems. The system is stable in all investigated scenarios. The detailed information of inputs is listed in Table I. For scenarios 1 and 2, uncertain resources include three loads and three PVs at buses 12, 15, and 16 and 13, 14, and 15, respectively; see Fig. 2. For the PCE method, the degree of expansion is set to be n=2 and the coefficients are calculated using the regression method with  $N_t = 100$  samples of rotor angle trajectories. The results of rotor angle  $\delta_{2-1}$  obtained from MCS are shown in Fig. 3 for illustrations, where upper and lower bounds are obtained using  $3\sigma$  rule. It can be observed that the trajectories scatter with different degrees of aggregation and the uncertainties from inputs can lead to quite different dynamic responses of the system. The comparisons results for different methods under scenarios 1 and 2 are displayed in Figs. 4 and 5. It can be found that the presence of different levels of linear correlation will affect the system responses. In particular, the variance for the response has been increased for the higher correlation scenario. Furthermore, the PCE model that ignores PVs correlations yields much larger errors as compared to other

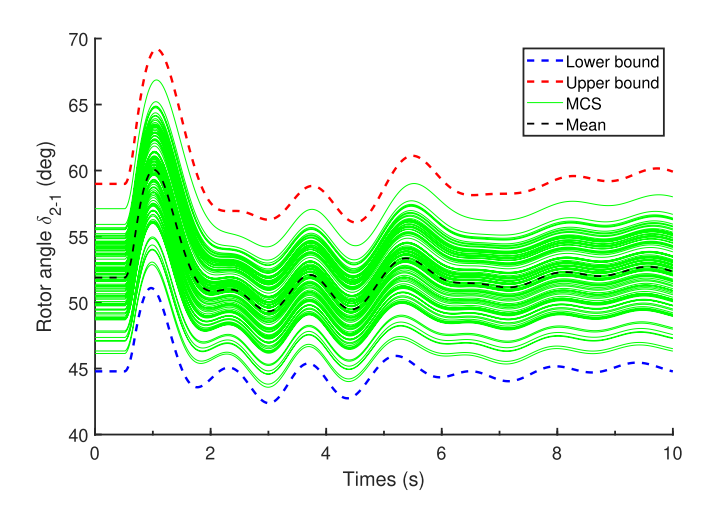


Fig. 3. Upper and lower bounds of rotor angle  $\delta_{2-1}$  in Scenario 1.

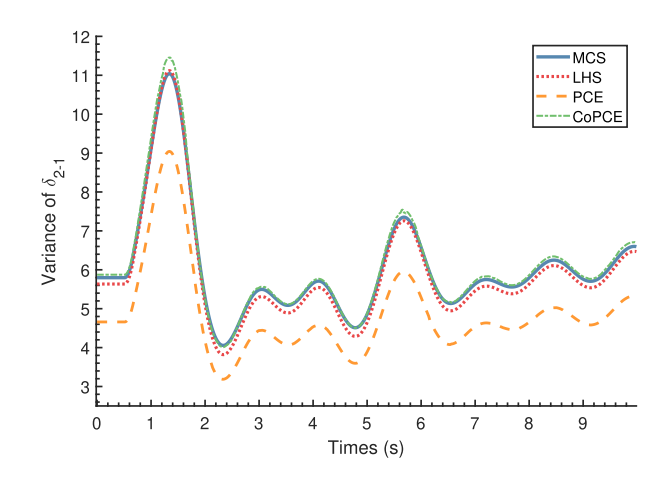


Fig. 4. Estimated variance of  $\delta_{2-1}$  by different methods for Scenario 1.

 $TABLE \ II \\ Comparison \ Results \ Among \ Different \ Methods \ for \ Scenarios \ 1 \ and \ 2 \\$ 

Scenario	Method	Accurace $e_{\mu}(\times 10^{-2}\%)$	CPU time (s)	
	MCS	_	_	220.72
Scenario 1	LHS	5.04	2.63	61.93
Scenario 1	PCE	3.20	19.65	14.01
	CoPCE	3.79	1.06	14.42
	MCS	_	-	217.28
Scenario 2	LHS	4.96	2.27	62.58
	PCE	5.38	30.31	14.20
	CoPCE	5.40	0.88	14.68

methods. CoPCE achieves similar performance as the benchmark MCS and outperforms LHS by around 1%. According to Table II, CoPCE has a much higher computational efficiency than LHS and MCS, i.e., CoPCE obtains 15 times faster than MCS and two times faster than LHS.

As demonstrated in Section III-A, the choice of PCE degree can affect both efficiency and accuracy. If the degree is increased to n=3, the error  $e_{\sigma^2}$  will drop off from 1.06% to 0.89%. However, the CPU time will increase from 14.42 to 20.56 s.

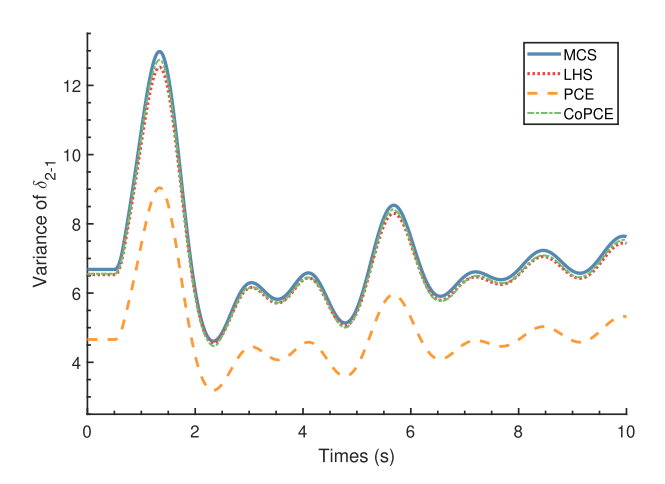


Fig. 5. Estimated variance of  $\delta_{2-1}$  by different methods for Scenario 2.

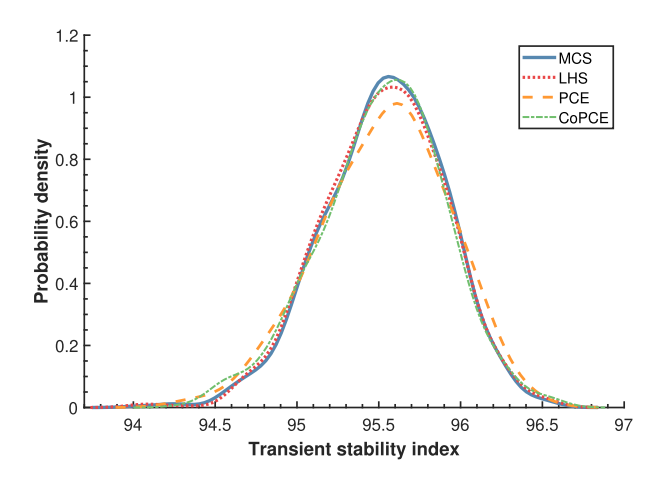


Fig. 6. Estimated PDF of TSI by different methods for Scenario 3.

Hence, the degree 2 is chosen for the experiments. For stable cases on the 39-bus system, Fig. 6 shows the estimated PDF of TSI. This confirms that all cases are stable and the TSI values are large, indicating a large stability margin.

#### B. Impacts of Uncertain Inputs With Nonlinear Correlations

This section investigates the impacts of nonlinear correlations of PVs on the dynamic responses. The number of inputs and their corresponding distributions for Scenarios 3 and 4 are the same as those in Scenarios 1 and 2. In Scenario 5, there are six loads and six PVs located at buses 12, 15, 16, 18, 21, and 23 and 13–17 and 19, respectively. The dependence structures for Scenarios 4-6 are described by C-Vine copula [22] and their types and parameters are shown in Table III. The parameters for LHS and PCE models are unchanged. Figs. 7 and 8 show the results for Scenarios 3 and 4, respectively, where copula is utilized to describe the nonlinear dependence among PVs. It can be found that the traditional PCE model is inadequate for handling nonlinear correlations among uncertain inputs as it yields rather large estimation errors. When the degree of nonlinear correlation increases, i.e., scenarios 3 and 4, the variance for the response also increases. The reason is that with an increased degree of

TABLE III
NONLINEAR CORRELATIONS OF PVS FOR SCENARIOS 3–7

Scenarios	Pair Copula type	Parameter
Scenario 3	[Clayton, Clayton, Clayton]	[1.5, 1, 0.5]
Scenario 4	[Clayton, Gumbel, Gumbel]	[3, 3, 1.2]
Scenario 5	[Clayton, Gumbel, Gumbel, Frank, Clayton, Clayton, Gumbel, Gumbel, Frank, Clayton, Clayton, Gumbel,	$ \begin{bmatrix} 2, 2, 1.2 \\ 0.8, 0.5, 2, \\ 2, 1.2, 0.8, \\ 0.5, 2, 2, \end{bmatrix} $
	Gumbel, Frank, Clayton]	1.2, 0.8, 0.5]
Scenario 6	[Clayton, Clayton, Clayton]	[1.5, 1, 0.5]
Scenario 7	$[Clayton, Clayton, Gumbel, Frank, t, \\ [Clayton, Clayton, Gumbel, Frank, t, ]$	

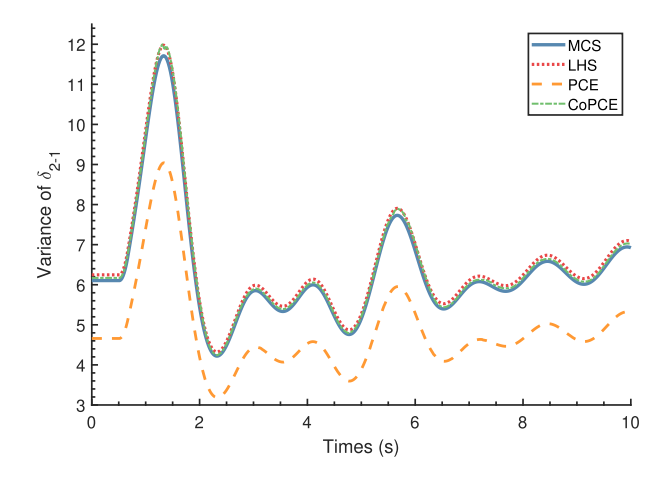


Fig. 7. Estimated variance of  $\delta_{2-1}$  by different methods for Scenario 3.

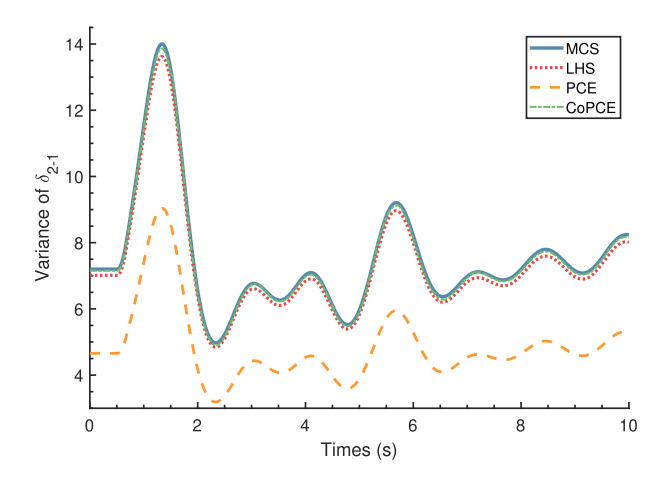


Fig. 8. Estimated variance of  $\delta_{2-1}$  by different methods for Scenario 4.

nonlinear correlations, the dynamic interactions among uncertain inputs are increased, leading to a more complicated dynamic system model response. The proposed CoPCE still achieves very high accuracy as compared to the benchmark MCS but is much more computationally efficient; see Table IV. When the number of uncertain inputs is further increased in Scenario 6, the variance of model response becomes larger; see Fig. 9. This is expected

TABLE IV	
COMPARISON RESULTS OF SCENARIOS 3-	5

Scenario	Method	Accurace $e_{\mu}(\times 10^{-2}\%)$	CPU time ((s))	
	MCS	-	_	223.01
Scenario 3	LHS	4.41	2.34	65.48
Scenario 3	PCE	4.24	23.67	15.19
	CoPCE	4.82	1.20	15.56
	MCS	_	-	224.71
Scenario 4	LHS	5.03	2.61	66.20
Scenario 4	PCE	1.21	35.36	15.43
	CoPCE	1.13	0.86	15.70
	MCS	_	-	227.28
Scenario 5	LHS	7.38	2.27	68.52
	PCE	12.50	30.31	28.46
	CoPCE	9.32	1.31	29.11

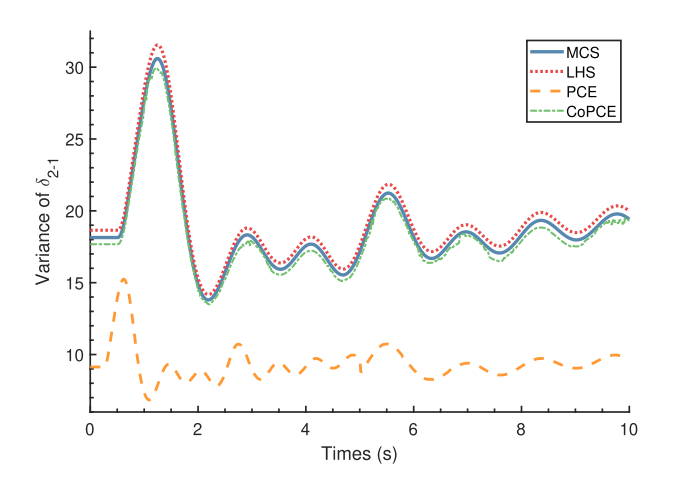


Fig. 9. Estimated variance of  $\delta_{2-1}$  by different methods for Scenario 5.

since more uncertainties in the inputs, more uncertainties occur for the model responses. The proposed CoPCE is able to accurately quantify that with a high computational efficiency.

#### C. Coexistence of Stable and Unstable Cases

This section aims to show that the proposed method can deal with the case, where stable and unstable cases coexist due to the uncertain inputs, i.e., Scenario 6. The parameter settings of uncertain inputs are the same as Scenario 3 but with different fault duration. As fault duration increases, the system tends to be unstable. Specifically, the fault duration is extended to 15 cycles and the system loading level is increased. The parameters for LHS and PCE methods are unchanged. The results are shown in Fig. 10 and it is very interesting to notice that due to uncertain inputs, both stable and unstable cases occur. In this case, a single PCE model is insufficient to capture the features of two kinds of trajectories. This justifies the development of the preprocessing strategy, where the trajectories are first classified into stable and unstable cases. One PCE model is constructed for each case. This is feasible because the statistical information of model response is inherent in PCE coefficients.

The PDF of TSI is shown in Fig. 11 and it can be observed that, in most cases, the TSI is larger than 0, while in some cases, the

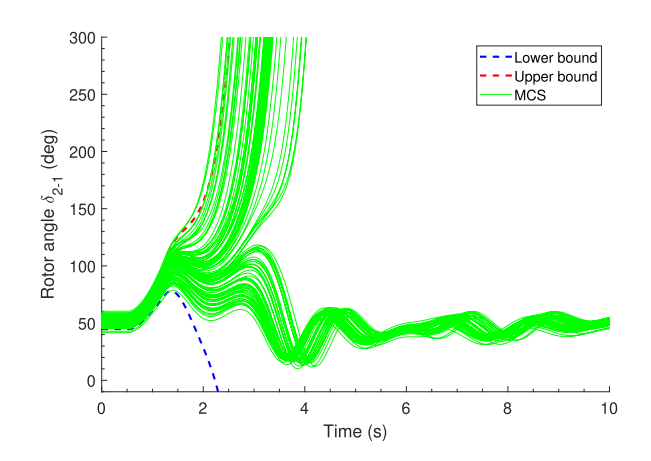


Fig. 10. MCS results of  $\delta_{2-1}$  where both stable and unstable cases coexist.

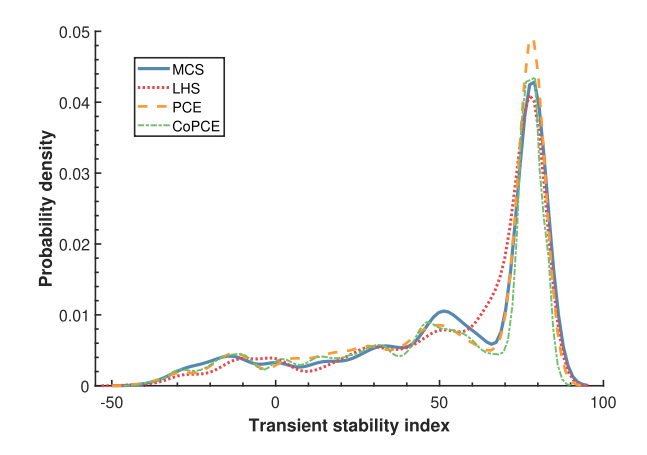


Fig. 11. Estimated PDF of TSI by different methods for Scenario 6.

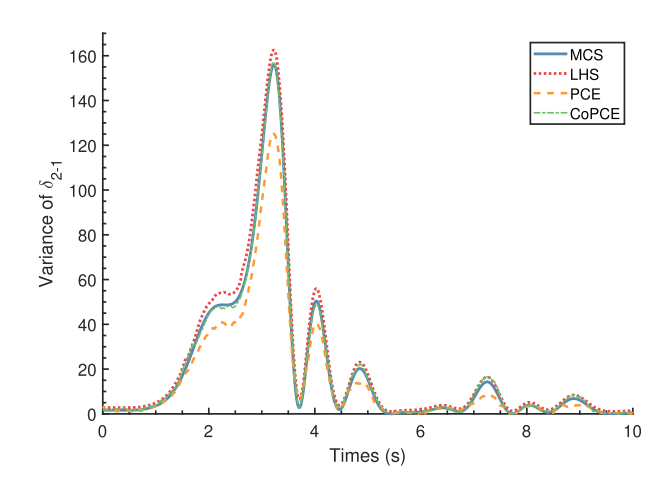


Fig. 12. Estimated variance of  $\delta_{2-1}$  by different methods for stable cases.

system is unstable, i.e., TSI value being less than 0. This provides critical information for enhancing system operators' awareness of the system instability risk and its degree. It is worth noting that the original PCE cannot handle the coexistence of stable and unstable scenarios if the proposed classification strategy is not used. Figs. 12 and 13 and Table V demonstrate that the

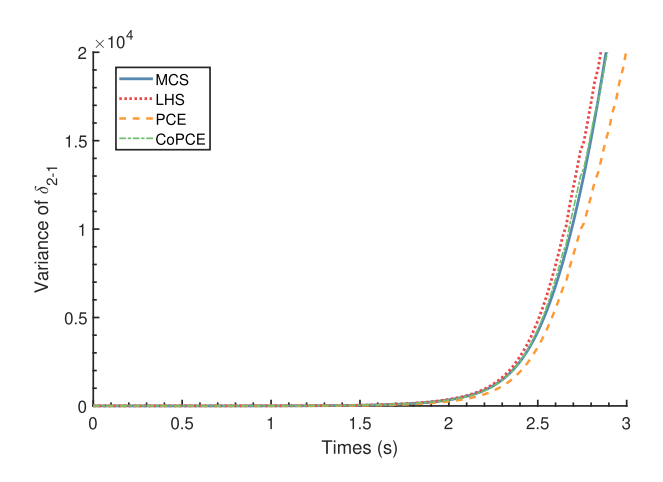


Fig. 13. Estimated variance of  $\delta_{2-1}$  by different methods for unstable cases.

TABLE V
COMPARISON RESULTS OF DIFFERENT METHODS UNDER SCENARIO 6

Scenario	Method	Accurace $e_{\mu}(\times 10^{-2}\%)$	CPU time (s)	
Scenario 6	MCS	_	_	225.69
	LHS	7.38	2.85	67.93
	PCE	24.98	48.88	28.56
	CoPCE	13.12	2.31	30.08

proposed CoPCE method can obtain excellent results for stable and unstable cases. For stable cases, the trajectories become rather complicated. After about 3 s, PCE models suffer from performance degradation. This is because the model that needs to be approximated becomes more complicated and the approximation error continuously accumulates as the simulation proceeds. In addition, for unstable cases, it is even more challenging to quantify. The main insight from this section is that the proposed method allows quantifying both stable and unstable cases while achieving the highest computational efficiency among all other methods.

#### D. Scalability to the Larger Scale System

The proposed method is also conducted on the modified IEEE 118-bus system with 30 uncertain inputs to test its scalability. As Scenario 7, the 30 uncertain sources include 15 loads and 15 PVs located at buses [11, 12, 14, 44, 45, 46, 47, 49, 66, 75, 77, 78, 80, 94, 96] and buses [7, 11, 17, 43, 45, 47, 67, 68, 71, 81, 93, 94, 95, 96, 97], respectively. The rotor angle of generator at bus 69 is selected for demonstration. The parameters of PCE methods are the same as those in Section IV except the number of observations for PCE is increased to  $N_t = 300$  due to a more complicated system and increased number of uncertain inputs. Total five PVs grouped at buses 93-97 are assumed to have nonlinear correlations and the parameters of the copula function are listed in Table III, i.e., Scenario 7. The simulation results are shown in Fig. 14 and Table VI. It can be found from Fig. 14 that the variance of the output gradually converges and CoPCE outperforms LHS and PCE. Table VI shows that CoPCE has

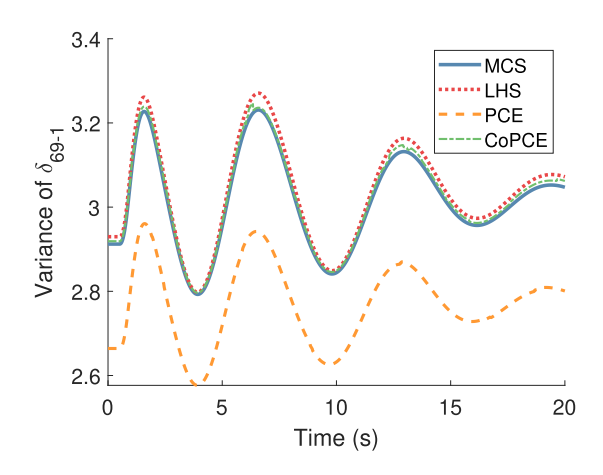


Fig. 14. Estimated variance of  $\delta_{69-1}$  by different methods for Scenario 7.

TABLE VI COMPARISON RESULTS OF DIFFERENT METHODS UNDER SCENARIO 7

Scenario	Method	Accurace $e_{\mu}(\times 10^{-2}\%)$	CPU time (s)	
Scenario 7	MCS	-	_	649.01
	LHS	3.23	2.05	185.19
	PCE	4.61	8.12	126.19
	CoPCE	1.92	1.27	123.24

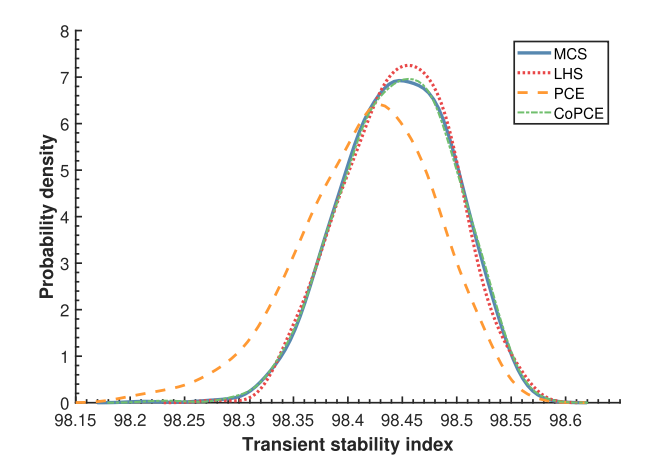


Fig. 15. Estimated PDF of TSI by different methods for Scenario 7.

the best performance with the least CPU time. The reason that CoPCE is faster than PCE might be the difficulties in getting the regression coefficients during the model construction stage due to the independent assumption of uncertain inputs. The TSI PDF is presented in Fig. 15 and it can be concluded that the system is stable as the proposed method shows the closest outcomes to MCS.

#### E. Validations With Dynamic PVs and Loads

In the previous tests, loads are assumed to be constant impedance, a widely used assumption for transient stability analysis. Since we are interested in electromechanical oscillations

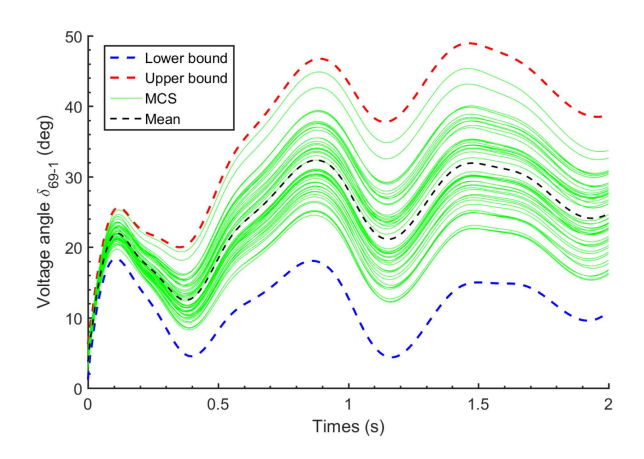


Fig. 16. Upper and lower bounds of rotor angle  $\delta_{69-1}$  in Scenario 8.

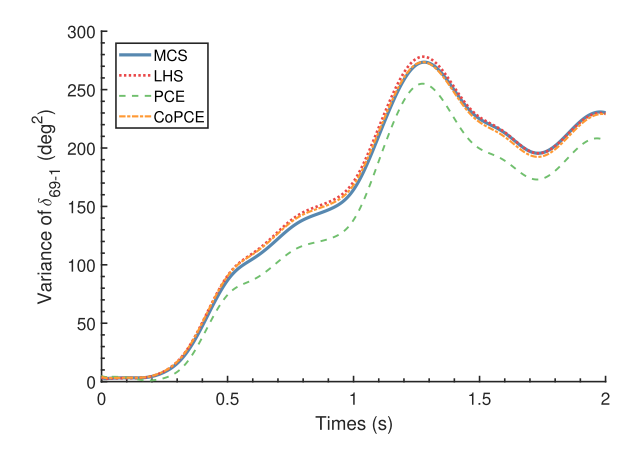


Fig. 17. Estimated variance of  $\delta_{69-1}$  by different methods for Scenario 8.

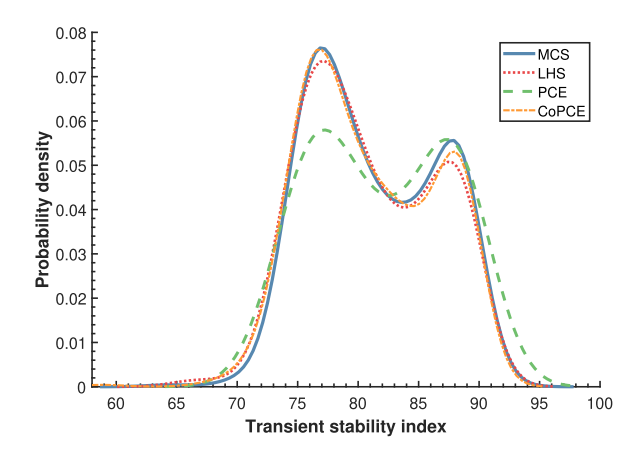


Fig. 18. Estimated PDF of TSI by different methods for Scenario 8.

(rotor angle stability), the fast dynamics of PVs are neglected. To further validate the effectiveness of the proposed method in handling dynamic loads and PVs, the composite dynamic load model and the dynamic PV model in [28] are tested. Specifically, the system is based on Section IV-D except that PVs and loads are modeled with the dynamic model. The dynamic representation

TABLE VII COMPARISON RESULTS OF DIFFERENT METHODS UNDER SCENARIO 8

Scenario	Method	Accurace $e_{\mu}(\times 10^{-2}\%)$	CPU time (s)	
Scenario 8	MCS	_	_	2419.95
	LHS	5.81	3.84	679.55
	PCE	5.90	16.24	131.61
	CoPCE	2.24	1.39	137.40

of the PV model can be found in [28], while the composite induction motor+ZIP dynamic load 20% induction motor is used for loads. The dynamic responses of the rotor angle  $\delta_{69-1}$  are shown in Fig. 16. As compared to the previous case, due to the dynamic PV and loads, the system responses are more complicated. Fig. 17 shows that the proposed method is able to effectively dynamic PVs. It can be found that the variance of rotor angle becomes larger, indicating a relatively larger fluctuation. Fig. 18 displays the probabilistic TSI. It is clear that the proposed method can still accurately quantify the system stability. It is interesting to note that with more complicated models, LHS has significantly reduced computational efficiency than our proposed method; see Table VII. This signifies the advantages of the proposed method over other sampling-based approaches.

#### V. CONCLUSION

In this article, a copula-PCE framework is proposed to quantify the uncertainties of power system dynamic results and stability assessment caused by uncertain loads and PVs. The impacts of linear and nonlinear correlations among PVs on the system dynamic behaviors are also investigated. The copula statistics are utilized to accurately characterize the dependence structure of PVs and the copula-PCE is employed for uncertainty quantification. To address the cases, where both stable and unstable conditions coexist, a preprocessing step via sample classification is proposed. The probabilistic TSI is developed and its PDF is estimated via kernel estimator. Extensive comparison results with MCS, LHS, and traditional PCE carried out on the modified IEEE 39- and 118-bus systems show that the proposed method is able to effectively deal with different uncertain input distributions and correlations, coexistence of stable and unstable cases, and dynamic PVs and loads while being computationally efficient.

In our article, the uncertainties come from power injections of uncertain loads and PVs and they belong to epistemic uncertainty [29]. Since the proposed framework is general, uncertainties from other sources can be handled as long as they are modeled appropriately, which can be done by defining proper input and output noise, measurement bias, model error, or random behavior of the system. In our future work, we will extend it to consider both aleatory and epistemic uncertainties. Note that more uncertain sources mean a higher dimension of input and larger computational cost. This may require the development of better sparse PCE methods.

## APPENDIX A MATHEMATICAL REPRESENTATION OF THE TWO-AXIS GENERATOR MODEL

TABLE VIII GENERATOR PARAMETER DATA [24]

No.	H	$R_a$	$x'_d$	$x'_q$	$x_d$	$x_q$	$T'_{d0}$	$T'_{q0}$	$x_l$
1	500	0	0.006	0.008	0.02	0.019	7	0.8	0.003
2	30.3	0	0.07	0.17	0.29	0.282	6.6	1.5	0.035
3	35.8	0	0.053	0.088	0.25	0.237	5.7	1.5	0.03
4	28.6	0	0.044	0.166	0.26	0.258	5.7	1.5	0.03
5	26	0	0.132	0.166	0.67	0.62	5.4	0.44	0.054
6	34.8	0	0.05	0.081	0.25	0.241	7.3	0.4	0.022
7	26.4	0	0.049	0.186	0.3	0.292	5.7	1.5	0.032
8	24.3	0	0.057	0.091	0.29	0.28	6.7	0.41	0.028
9	34.5	0	0.057	0.059	0.21	0.205	4.8	2	0.03
10	42	0	0.031	0.08	0.1	0.069	10	0	0.013

The differential and algebraic equations of the ninth-order two-axis generator model with IEEE-DC1A exciter and TGOV1 turbine-governor are represented as follows.

Differential Equations

$$T'_{do}\frac{dE'_q}{dt} = -E'_q - (X_d - X'_d)I_d + E_{fd}$$
 (15)

$$T'_{qo}\frac{dE'_d}{dt} = -E'_d - (X_q - X'_q)I_q$$
 (16)

$$\frac{d\delta}{dt} = \omega - \omega_s \tag{17}$$

$$\frac{2H}{\omega_s}\frac{d\omega}{dt} = T_M - P_e - D\left(\omega - \omega_s\right) \tag{18}$$

$$T_E \frac{dE_{fd}}{dt} = -(K_E + S_E(E_{fd})) E_{fd} + V_R$$
 (19)

$$T_{\rm F} \frac{dV_F}{dt} = -V_F + \frac{K_F}{T_E} V_R - \frac{K_F}{T_E} \left( K_E + S_E \left( E_{fd} \right) \right) E_{fd}$$
(20)

$$T_A \frac{dV_R}{dt} = -V_R + K_A \left( V_{\text{ref}} - V_F - V \right) \tag{21}$$

$$T_{CH}\frac{dT_M}{dt} = -T_M + P_{SV} \tag{22}$$

$$T_{SV}\frac{dP_{SV}}{dt} = -P_{SV} + P_C - \frac{1}{R_D}\left(\frac{\omega}{\omega_0} - 1\right)$$
 (23)

where  $T_{do}'$ ,  $T_{qo}'$ ,  $T_E$ ,  $T_F$ ,  $T_A$ ,  $T_{CH}$ , and  $T_{SV}$  are time constants;  $K_E$ ,  $K_F$ , and  $K_A$  are controller gains;  $V_{\rm ref}$  and  $P_C$  are known control inputs;  $E_q'$ ,  $E_d'$ ,  $E_{fd}$ ,  $V_F$ ,  $V_R$ ,  $T_M$ , and  $P_{SV}$  are the q-and d-axes transient voltages, field voltage, scaled output of the stabilizing transformer and scaled output of the amplifier, synchronous machine mechanical torque, and steam valve position, respectively;  $X_d$ ,  $X_d'$ ,  $X_q$ , and  $X_q'$  are generator parameters; V is the terminal bus voltage magnitude; and  $I_d$  and  $I_q$  are the d-and q-axes currents, respectively.

Algebraic equations

$$V_d = V \sin(\delta - \theta), V_d = V \cos(\delta - \theta) \tag{24}$$

$$I_d = \frac{E'_q - V_q}{X'_d}, I_q = \frac{V_d - E'_d}{X'_q}$$
 (25)

$$P_e = V_d I_d + V_q I_q, Q_e = -V_d I_q + V_q I_d$$
 (26)

where  $V_d$  and  $V_q$  are the d- and q-axes voltage magnitudes, and  $\theta$  is the terminal bus voltage phase angle; and  $P_e$  and  $Q_e$  are the active and reactive electrical power outputs, respectively. The generator parameters are displayed in Table VIII.

#### REFERENCES

- [1] Y. C. Chen and A. D. Domínguez-García, "A method to study the effect of renewable resource variability on power system dynamics," *IEEE Trans. Power Syst.*, vol. 27, no. 4, pp. 1978–1989, Nov. 2012.
- [2] S. Q. Bu, W. Du, and H. F. Wang, "Probabilistic analysis of small-signal rotor angle/voltage stability of large-scale AC/DC power systems as affected by grid-connected offshore wind generation," *IEEE Trans. Power* Syst., vol. 28, no. 4, pp. 3712–3719, Nov. 2013.
- [3] J. C. Muñoz, C. A. Cañizares, K. Bhattacharya, and A. Vaccaro, "An affine arithmetic based method for voltage stability assessment of power systems with intermittent generation resources," *IEEE Trans. Power Syst.*, vol. 28, no. 4, pp. 4475–4487, Nov. 2013.
- [4] R. Prece and J. V. Milanović, "Assessing the applicability of uncertainty importance measures for power system studies," *IEEE Trans. Power Syst.*, vol. 31, no. 3, pp. 2076–2084, May 2016.
- [5] J. L. Rueda, D. G. Colome, and I. Erlich, "Assessment and enhancement of small signal stability considering uncertainties," *IEEE Trans. Power Syst.*, vol. 24, no. 1, pp. 198–207, Feb. 2009.
- [6] T. Odun-Ayo and M. L. Crow, "Structure-preserved power system transient stability using stochastic energy functions," *IEEE Trans. Power Syst.*, vol. 27, no. 3, pp. 1450–1458, Aug. 2012.
- [7] S. V. Dhople, Y. C. Chen, L. DeVille, and A. D. Domínguez-García, "Analysis of power system dynamics subject to stochastic power injections," *IEEE Trans. Circuits Syst. I., Reg. Papers*, vol. 60, no. 12, pp. 3341–3353, Dec. 2013.
- [8] D. A. Maldonado, M. Schanen, and M. Anitescu, "Uncertainty propagation in power system dynamics with the method of moments," in *Proc. IEEE Power Energy Soc. Gen. Meeting*, Portland, OR, USA, 2018, pp. 1–5.
- [9] H. Choi, P. J. Seiler, and S. V. Dhople, "Propagating uncertainty in powersystem DAE models with semidefinite programming," *IEEE Trans. Power Syst.*, vol. 32, no. 4, pp. 3146–3156, Jul. 2017.
- [10] L. Tang, "Dynamic security assessment processing system," Ph.D. dissertation, Dept. Elect. Comput. Eng., Iowa State Univ., Ames, IA, USA, 2014
- [11] P. Ju, H. Li, C. Gan, Y. Liu, Y. Yu, and Y. Liu, "Analytical assessment for transient stability under stochastic continuous disturbances," *IEEE Trans. Power Syst.*, vol. 33, no. 2, pp. 2004–2014, Mar. 2018.
- [12] T. Tian, X. Kestelyn, O. Thomas, H. Amano, and A. R. Messina, "An accurate third-order normal form approximation for power system non-linear analysis," *IEEE Trans. Power Syst.*, vol. 33, no. 2, pp. 2128–2139, Mar. 2018.
- [13] K. Hua, Y. Mishra, and G. Ledwich, "Fast unscented transformation-based transient stability margin estimation incorporating uncertainty of wind generation," *IEEE Trans. Sustain. Energy*, vol. 6, no. 4, pp. 1254–1262, Oct. 2015.
- [14] J. R. Hockenberry and B. C. Lesieutre, "Evaluation of uncertainty in dynamic simulations of power system models: The probabilistic collocation method," *IEEE Trans. Power Syst.*, vol. 19, no. 3, pp. 1483–1491, Aug. 2004.
- [15] Y. Xu, L. Mili, A. Sandu, M. R. v. Spakovsky, and J. Zhao, "Propagating uncertainty in power system dynamic simulations using polynomial chaos," *IEEE Trans. Power Syst.*, vol. 34, no. 1, pp. 338–348, Jan. 2019.
- [16] W. Wu, K. Wang, B. Han, G. Li, X. Jiang, and M. L. Crow, "A versatile probability model of photovoltaic generation using pair copula construction," *IEEE Trans. Sustain. Energy*, vol. 6, no. 4, pp. 1337–1345, Oct. 2015.
- [17] K. Ye, J. Zhao, R. Yang, Y. Zhang, and X. Liu, "A generalized copulapolynomial chaos expansion for probabilistic power flow considering nonlinear correlations of PV injections," in *Proc. 52nd North Amer. Power Symp.*, 2021, pp. 1–6.
- [18] K. Ye, J. B. Zhao, N. Duan, and D. Adrian Maldonado, "Uncertainty quantification of loads and correlated PVs on power system dynamic simulations," *IEEE IAS Ind. Commercial Power System Asia*, 2021, pp. 44–49.
- [19] D. Xiu, Numerical Methods for Stochastic Computations: A Spectral Method Approach. Princeton, NJ, USA: Princeton Univ. Press, 2010.

- [20] M. Gerritsma, J. van der Steen, P. Vos, and G. Karniadakis, "Time-dependent generalized polynomial chaos," *J. Comput. Phys.*, vol. 229, no. 22, pp. 8333–8363, Nov. 2010.
- [21] S. Marelli, N. Luthen, and B. Sudret, "UQLab user manual—Polynomial chaos expansions," Chair of Risk, Safety and Uncertainty Quantification, ETH Zurich, Switzerland, Tech. Rep. UQLab-V1.4-104, Feb. 2021.
- [22] E. Torre, S. Marelli, P. Embrechts, and B. Sudret, "A general framework for data-driven uncertainty quantification under complex input dependencies using vine copulas," *Probabilistic Eng. Mech.*, vol 55, pp. 1–16, 2019.
- [23] M. Sun, I. Konstantelos, and G. Strbac, "C-vine copula mixture model for clustering of residential electrical load pattern data," *IEEE Trans. Power* Syst., vol. 32, no. 3, pp. 2382–2393, May 2017.
- [24] C. Canizares et al., "Benchmark systems for small-signal stability analysis and control," IEEE Power Energy Soc., Piscataway, NJ, USA, Tech. Rep. PES-TR18, Aug. 2015.
- [25] J. V. Milanović, "Probabilistic stability analysis: The way forward for stability analysis of sustainable power systems," *Philos. Trans. Roy. Soc. A, Math., Phys. Eng. Sci.*, vol. 375, no. 2100, Jul. 2017, Art. no. 20160296.
- [26] M. P. Wand and M. C. Jones, Kernel Smoothing. London, U.K.: Chapman & Hall, 1995.
- [27] R. Preece and J. V. Milanović, "Efficient estimation of the probability of small-disturbance instability of large uncertain power systems," *IEEE Trans. Power Syst.*, vol. 31, no. 2, pp. 1063–1072, Mar. 2016.
- [28] WECC Renewable Energy Modeling Task Force, "WECC PV power plant dynamic modeling guide," Western Electricity Coordinating Council, Salt Lake City, UT, USA, Apr. 2014.
- [29] J. Teh, "Uncertainty analysis of transmission line end-of-life failure model for bulk electric system reliability studies," *IEEE Trans. Rel.*, vol. 67, no. 3, pp. 1261–1268, Sep. 2018.